Scientific Research Publishing

Journal of High Energy Physics, Gravitation and Cosmology, 2024, 10, 749-774
https://www.scirp.org/journal/jhepgc
ISSN Online: 2380-4335
ISSN Print: 2380-4327

The Origin, Properties and Detection of Dark Matter and Dark Energy

Sylwester Kornowski

(Retired) Physics Poznań University (UAM), Szczecin, Poland
Email: sylwester.kornowski@gmail.com

How to cite this paper: Kornowski, S. (2024) The Origin, Properties and Detection of Dark Matter and Dark Energy. *Journal of High Energy Physics, Gravitation and Cosmology*, **10**, 749-774.
https://doi.org/10.4236/jhepgc.2024.102046

Received: February 1, 2024
Accepted: April 20, 2024
Published: April 23, 2024

Abstract

The pictures from the James Webb Space Telescope (JWST) suggest that massive galaxies were already at the beginning of the expansion of the Universe because there was too short time to create them. It is consistent with the new cosmology presented within the Scale-Symmetric Theory (SST). The phase transitions of the initial inflation field described in SST lead to the Protoworld—its core was built of dark matter (DM). We show that the DAMA/LIBRA annual-modulation amplitude forced by the change of the Earth's velocity (*i.e.* baryonic-matter (BM) velocity) in relation to the spinning DM field in our Galaxy's halo should be very low. We calculated that in the DM-BM weak interactions are created single and entangled spacetime condensates with a lowest mass/energy of 0.807 keV—as the Higgs boson they can decay to two photons, so we can indirectly detect DM. Our results are consistent with the averaged DAMA/LIBRA/COSINE-100 curve describing the dependence of the event rate on the photon energy in single-hit events. We calculated the mean dark-matter-halo (DMH) mass around quasars, we also described the origin of the plateaux in the rotation curves for the massive spiral galaxies, the role of DM-loops in magnetars, the origin of CMB, the AGN-jet and galactic-halo production, and properties of dark energy (DE).

Keywords

New Cosmology, Dark Matter, DM-BM Weak Interactions, DMH Mass around Quasars, Rotation Curves of Galaxies, Magnetars, CMB, AGN-Jet Production, Galactic-Halo Production, Dark Energy

1. Introduction

The dark matter (DM) and dark energy (DE) problems can be, in principle, achieved by extending the general theory of relativity (GR)—this is stressed, for

example, in [1]. We know that the combination of the geometric description of the Newton's gravity with the Einstein's special relativity leads to GR. The Einstein's equations describe the relation between the geometry of four-dimensional spacetime and the energy-momentum contained in the spacetime. On the other hand, in the Scale-Symmetric Theory (SST), there is the two-component spacetime [2]. There is the SST Higgs field (SST-Hf) composed of the non-gravitating tachyons with infinitesimal spins (mean spin is approximately 67 orders of magnitude lower than the reduced Planck constant) and there is the SST absolute spacetime (SST-As) composed of the spin-1 objects moving with the speed $c \approx 3\times 10^{8}\,\mathrm{m}\cdot\mathrm{s}^{-1}$. Generally, SST leads to GR but the two-component spacetime causes that in SST, there appear new phenomena that lead to the origin of DM and DE.

We need a theory of nature that starts from the true internal structure of spacetime—SST is such a theory [2]. The phase transitions of the initial inflation field described in SST lead to new cosmology via the Protoworld [2].

The origin of the matter-antimatter asymmetry is as follows. In SST, to explain the matter-antimatter asymmetry, we assumed that the initial inflation field (*i.e.* the SST initial Higgs field composed of superluminal pieces of space without internal structure packed to maximum), as a whole, had lefthanded helicity, *i.e.* there was the lefthanded helical motion. Such motion, due to a collision (the SST big bang), transformed into the lefthanded internal helicity of the massive protons and neutrons and, to conserve the resultant electric charge, into the righthanded internal helicity of the light electrons, so the resultant helicity of the protons, neutrons and electrons is lefthanded. The resultant internal helicity of the antiprotons, antineutrons and positrons (*i.e.* of antimatter) is righthanded, so baryonic matter dominates in our Cosmos.

Of course, the first to be created, in the dominant number, were the neutrino-antineutrino pairs (and other particles with much lower number density) that are the components of the SST absolute spacetime (SST-As), composed of the binary systems of the closed strings (they are the SST superluminal entanglons that are responsible for the quantum entanglement), but due to the internal structure of the entanglons and neutrinos at this level, the matter-antimatter symmetry was not broken.

The torus/physical-loop is the simplest object that can have internal helicity, so tori were and are everywhere, *i.e.* in the Protoworld, inside the black holes (BHs) when they are surrounded by accretion disc, around the BHs in the active galactic nuclei (AGN), in fermions, and so on.

The tori have the toroidal and poloidal motions and to stabilize them, there appear the radial motions that lead to creation of the central condensate.

A condensate or a torus can be a black hole not only because of gravitational interactions but also because of the nuclear weak interactions or nuclear strong interactions.

Symmetrical decays of the strong (S) or electroweak (EW) virtual fields produced by BHs cause that around them can be valid the Titius-Bode (TB) law.

In SST, we use the quantum entanglement and special theory of relativity but we can avoid the formalism of the Quantum Mechanics because we formulated and apply the dynamics of statistical distributions of enormous number of classical or classical and quantum particles—it concerns the baryons in AGN, the SST absolute-spacetime components in hadrons and charged leptons, the entanglons in neutrinos, the DM-tori in the Protoworld, and so on [2].

Such distributions are similar. There is a torus/physical-loop with a central condensate to conserve stability of the torus and there can be an accretion disc(s) and sometimes there can be valid the Titius-Bode law.

In SST, the nucleons (p and n) consist of the core (there is the torus/electric-charge that is responsible for the electromagnetic interactions via photons and for the nuclear-strong interactions via gluons, and there is the central spacetime condensate, Y, that is responsible for the weak interactions) and outside the core, but below the Schwarzschild surface for the nuclear strong interactions, there is a relativistic pion interacting with the baryonic core due to the nuclear strong interactions [2].

The origin of dark matter and dark energy is as follows.

As SST shows, to create the core of the Protoworld, the same in shape but not size to both the core of neutrinos and the core of baryons, we need a stable particle with a mass equal to mass of the charged core of baryons, *i.e.* $H^+ = 727.4392$ MeV, so it cannot be a nucleon. In SST, we showed that it is the dark-matter torus ($M_{DM\text{-}torus} = H^+$) composed of the SST-As components [2]. Such DM-torus consists of the entangled DM-loops with the invariant mass $M_{DM\text{-}loop} = 1.16656 \times 10^{-11}$ eV [2].

In DM-loops, the spins of the SST-As components are tangent to the loops (in the photon loops, the spins are perpendicular to the loops), so the DM-loops and DM-tori cannot interact electromagnetically—they can interact gravitationally and weakly.

The SST DM-loops consist of tremendous number of the non-rotating-spin neutrinos, so we should explain why mass of the DM loops is about 10 orders of magnitude lower than the experimental upper limit for the sum of the neutrino masses.

The P18 result for neutrinos from CMB is: $\left(\Sigma m_\nu\right)_{CMB} < 0.287$ eV (95% C.L.) [3]). On the other hand, the neutrino spin rotation decreases pressure in the SST absolute spacetime around the neutrinos—it causes that the SST absolute spacetime near the rotating-spin neutrinos is thickened, so their masses (the excited-state masses) are higher than the non-rotating-spin neutrinos (the ground-state mass ≈ 3.335×10^{-67} kg [2]).

Similarity of the core of Protoworld (it was built of the DM-tori) and the core of baryons gives us the opportunity to calculate the ratioof the mass of DM to mass of baryonic matter (BM), $F_{DM/BM}$, in our Universe. Since BM is an analogue to the neutral pion produced inside the core of baryons, so we have

$$F_{DM/BM} = \frac{H^+}{\pi^o} = \frac{727.44\ \text{MeV}}{134.98\ \text{MeV}} = 5.389\,. \tag{1}$$

The gravitational collapse of the core of the Protoworld forced the decays of the DM-tori into the DM-loops, so today abundance of the DM-tori should be very low while of the DM-loops very high.

The above remarks lead to the conclusion that to detect dark matter we should investigate the interactions of the DM-loops with the $Y = 424.12176$ MeV spacetime condensates in centres of baryons via the weak interactions of the virtual electron-positron pairs, *i.e.* the local DM-BM interactions via the leptonic weak interactions. The coupling constant for such local DM-BM interactions is

$$\alpha_{w(DM\text{-}BM)} = 2\alpha_{w(e)} = 1.902236 \times 10^{-6}, \quad (2)$$

where the factor 2 is due to the pair (not a single fermion), and $\alpha_{w(e)} = 0.951118 \times 10^{-6}$ is the weak coupling constant for electrons [2]. In this paper, we described detection of DM via such interactions.

Notice that due to evolution of the protogalaxies composed of the neutron black holes (NBHs—they were created already before the expansion of the Universe), the DM-loops had absorbed angular momentum of the protogalaxies, so, generally, their sizes increased to cosmological scales—the DM halos of the massive spiral galaxies are composed of such concentric cosmological DM-loops. The today sizes of the DM loops are mostly comparable in size to galactic halos, galaxy-cluster halos or closed galaxy-filament halos but their sizes can vary from ~0.5 fm to cosmological sizes. Emphasize that contrary to angular momentums of the DM-loops, mass of the DM-loops is invariant.

We see that today the SST dark matter is a cold field composed of the weakly and gravitationally interacting very light DM-loops with invariant mass.

We need dark energy (DE) to explain what sustains the expansion of the Universe, what caused the explosion of the Protoworld, and why the supernovae and other cosmological objects explode.

In SST, DE consists of the virtual photons/gluons from the annihilations of the virtual fermion-antifermion pairs, from decays of the virtual pions and virtual spacetime condensates (*i.e.* the scalar bosons), and so on.

The dynamics of the virtual fields is as follows. Nature tries to equalize the mass/energy density, so real particles that have positive mass create virtual fields that consists of the virtual "holes" that appear in the SST-As and virtual fields in the places of creation of the not moving virtual objects with positive mass. Dynamic pressure in SST-As is ~10^{45} Pa [2], so the part of a virtual field that is composed of the "holes", which have negative mass, very quickly becomes a smooth field (SST shows that the SST-As components have infinitesimal inertia), so the positive/attractive pressure from such virtual part appears only on the boundary of the virtual field. It means that the virtual photons/gluons behave in relation to the smooth field as the real energy, so there appears the negative/repulsive pressure $p_{DE} = -\rho_{DE}c^2$ —such is the origin of DE.

We see that DE tries to expand a system at the cost of the inflows of the SST-As forced by the positive pressure on the boundary of the virtual field—e.g., such a boundary is on the front of the expanding Universe. Notice that mass

density of the SST-As inside the Universe is a little lower than outside it.

In SST, we assume that the Protoworld was an analogue to the dipole state of the neutron, *i.e.* $H^{+}W_{(-),d=1}$, and that dark energy was an analogue to the positive mass of the virtual fields. On the circular axis of the torus in the core of the Protoworld there were the two baryonic loops. The core of the Protoworld was built of DM. According to SST, an analogue to the energy $W_{(-),d=1}$ was composed of photon loops overlapping with the $d = 1$ state.

To obtain the correct value of the anomalous magnetic moment of the electron, we must assume that there is created only one virtual electron-positron pair, *i.e.* the positive mass of the virtual field is two times higher than mass of the bare electron [2]. It follows from the fact that to create a mass M there must appear a massless energy $E = M$, so the total involved energy is $M + E = 2E$.

Mass of the $d = 1$ photon loops is zero but there is the positive mass of their virtual field that transforms into DE, so DE from the cosmological photon loops is proportional to $2W_{(-),d=1}$. On the other hand, initially the baryonic matter was cold, so its virtual nuclear strong fields were confined, *i.e.* they practically did not and do not produce DE. The virtual strong fields in cold BM do not annihilate into virtual photons that is the precondition to produce negative/repulsive pressure. Of course, each elementary charge creates one virtual bare electron-positron pair, so it concerns the proton as well, but mass of the virtual pair is much lower than mass of resting proton, so we can neglect DE from such pairs.

Emphasize that abundance of regions with hot baryonic matter was very low, so we can neglect DE from such regions. Such regions produced and produce virtual pions and other virtual systems that decay to virtual photons. Abundance of DE in such regions is increased. The CMB from such regions gives different results. It concerns higher angular scales (lower multipole momentums) in the CMB power spectrum.

For DE we have $E_{\Lambda} \sim 2\left(H^{+} + W_{(-),d=1}\right) = 1886.40$ MeV.

Cold dark matter was an analogue to mass of the core of the Protoworld, *i.e.* $M_c \sim H^{+} = 727.44$ MeV [2].

BM was an analogue to mass of the neutral pion, *i.e.* $M_b \sim \pi^{o} = 134.98$ MeV [2].

Introduce the symbol E_{total} that is proportional to the sum of DE and positive masses (we neglect DE from the confined virtual strong fields and the mass less energy of the $d = 1$ photon loops)

$$E_{total} \sim E_T = 2\left(H^{+} + W_{(-),d=1}\right) + H^{+} + \pi^{o} = 2748.82 \text{ MeV}. \quad (3)$$

Relative abundance of DE should be

$$\Omega_{\Lambda} = \frac{2\left(H^{+} + W_{(-),d=1}\right)}{E_T} = \frac{E_{\Lambda}}{E_{total}} = 0.6863 \quad i.e.\ 68.63\% \text{ of DE}. \quad (4)$$

Relative abundance of cold DM should be

$$\Omega_c = \frac{H^+}{E_T} = \frac{M_c}{E_{total}} = 0.2646 \quad i.e.\ 26.46\%\ \text{of cold DM.} \tag{5}$$

Relative abundance of BM should be

$$\Omega_b = \frac{\pi^o}{E_T} = \frac{M_b}{E_{total}} = 0.0491 \quad i.e.\ 4.91\%\ \text{of BM.} \tag{6}$$

The Particle Data Group (PDG) cosmological constants are as follows: 68.5(7)% of DE, 26.5(7)% of cold DM and 4.93(6)% of BM [4]. We see that the SST results (4)-(6) are perfect.

The WMAP 9-year results from the NASA/WMAP Science Team are as follows: DE: $71.35^{+0.92}_{-0.96}\%$, DM: $24.02^{+0.88}_{-0.87}\%$ and BM: 4.628% ± 0.093%:

(see https://map.gsfc.nasa.gov/media/121236/121236_NewPieChart.pdf).

The WMAP/NASA team measured temperature differences in CMB. They wrote a program based on known physics to generate artificial sky maps. Next they varied the ingredients to obtain the real CMB. Then, why the PDG cosmological constants [4] differ from the WMAP data?

SST shows that when we assume that BM creates DE (it is true at very high energies), *i.e.* $E_\Lambda \sim 2\left(H^+ + W_{(-),d=1} + \pi^o\right) = 2156.35\ \text{MeV}$ and $E_{total} \sim 2\left(H^+ + W_{(-),d=1} + \pi^o\right) + H^+ + \pi^o = 3018.77\ \text{MeV}$, then from (4)-(6) we obtain: 71.43% of DE, 24.10% of cold DM and 4.47% of BM—these results are in a perfect consistency with the WMAP/NASA results.

When we neglect the virtual fields then composition of the Universe is and was as follows: 67.5% of cold DM, 12.5% of BM and 20.0% of photon loops.

In SST, the SST-As components have spin equal to 1, so a neutral object that does not disturb the ground state of the SST spacetime (*i.e.* its spin and weak-charge are zero) must consists of four fermions/neutrinos—it leads to the 4-object/quadrupole symmetry. Objects have tendency to create binary systems, so at high-energies/early-Universe abundance of binary systems of quadrupoles should be highest (*i.e.* objects composed of 8 components). For example, abundance of quasars composed of 8 protogalaxies with invariant mass should be highest.

Due to the 4-object symmetry and saturation of interactions, the number of entangled components in a single object can be

$$N_d = 4^d, \tag{7}$$

where $d = 0,1,2,4,8,16,32,\cdots$ are the Titius-Bode numbers [2].

According to SST, the protogalaxies created before the expansion of the Universe were built of NBHs with the invariant mass M_{NBH} that is 24.81 times higher than the mass of the Sun, M_{Sun}. Such a mass follows from the atom-like structure of baryons that leads to the effective distances of neutrons equal to $A + 4B = 2.7048\ \text{fm}$ (they are the diagonals of the faces of a cube), where $A = 0.6974425\ \text{fm}$ is the equatorial radius of the core of the baryons, and $B = 0.501835\ \text{fm}$ is the distance between the $d = 1$ state and the equator [2]. Radius of NBHs is invariant and is 36.64 km.

For protogalaxies, the only non-trivial TB number is $d=16$, so the invariant mass of the protogalaxies was (it is only the baryonic mass)

$$M_{Proto,BM}=4^{16}\times 24.81M_{Sun}=1.066\times 10^{11}M_{Sun}. \quad (8)$$

The nature of the interaction of dark matter with baryonic matter is one of unsolved cosmological problems. Detection of some spectrum related to the stellar orbital speeds in the halos of massive galaxies, such as the Milky Way, would shed light on the nature of DM and its origin. Unfortunately, the annual modulation in the DAMA/LIBRA experiment [5] has not been definitively confirmed in other experiments using the same NaI(Tl) target material [6] [7] [8] [9]. In SST, we have shown that this is due to the Earth's very low orbital speed relative to the spin speed of DM. SST shows that it is very difficult to detect the annual modulation because the orbital speed of the Earth (~30 km·s^{-1}) is very low in comparison with the spin speed of the SST DM loops (~3 × 10^5 km·s^{-1})—ratio of them is 10^4, so only in very sensitive measurements we can detect an annual modulation.

But the practically negative result concerning the annual modulation does not mean that the DM-BM interaction was not detected in the DAMA/LIBRA experiment. SST shows that we need to focus on the dependence of the event rate on the photon energy in single-hit events. In paper [6], we have a comparison of such a dependence obtained in the DAMA/LIBRA and COSINE-100 experiments.

2. Energies of the Spacetime Condensates and Photons from the DM-BM Interactions

The crystal used in the DAMA/LIBRA and COSINE-100 experiments is the thallium-doped sodium iodine (NaI(Tl)). From the model of dynamic supersymmetry for atomic nuclei we have

$$^{23}_{11}\mathrm{Na}\equiv 2(4\mathrm{p}4\mathrm{n})+1(3\mathrm{p}4\mathrm{n}), \quad (9)$$

$$^{127}_{53}\mathrm{I}\equiv 5(4\mathrm{p}4\mathrm{n})+10(3\mathrm{p}5\mathrm{n})+1(3\mathrm{p}4\mathrm{n}), \quad (10)$$

$$^{205}_{81}\mathrm{Tl}\equiv 3(4\mathrm{p}4\mathrm{n})+21(3\mathrm{p}5\mathrm{n})+1(2\mathrm{p}2\mathrm{n})+1(3\mathrm{p}4\mathrm{n}). \quad (11)$$

We see that in the crystal, there dominate the cuboids composed of 8 nucleons, *i.e.* binary systems of quadrupoles of nucleons.

In the DM-nucleon interaction in a solid, there is produced a spacetime condensate with following mass/energy

$$E_C=\alpha_{w(DM\text{-}BM)}Y=0.807\ \mathrm{keV}. \quad (12)$$

The spacetime-condensates created in the core of baryons can decay to two photons (the same as the Higgs boson that is the spacetime condensate as well) each with energy of $\gamma\approx 0.4\ \mathrm{keV}$.

Due to the four-particle symmetry and the energy equilibrium for all types of the entangled spacetime condensates, there appear following photon fields.

***For single nucleons in the cuboids we have**

Field: γ (1 type); threshold energy: $E_{photon} = \gamma = 0.4$ keV

Our normalization is:

$$Rate\left(\text{counts/keV/kg/day}\right) = \frac{5\left(\text{see}\left(16\right)\right)}{1\,\text{type}}\left[\frac{1}{1}\right] = 5.0 \tag{13}$$

***For the bases of the cuboids (alpha particles)**

Field: $4\gamma + \gamma$ (2 types); threshold energy: $E_{photon} = 4\gamma = 1.6$ keV

$$Rate = \frac{5}{2\,\text{types}}\left[\frac{1}{1} + \frac{1}{4}\right] = 3.1 \tag{14}$$

***For cuboids**

Field: $8\gamma + 4\gamma + \gamma$ (3 types); threshold energy: $E_{photon} = 8\gamma = 3.2$ keV

$$Rate = \frac{5}{3\,\text{types}}\left[\frac{1}{1} + \frac{1}{4} + \frac{1}{8}\right] = 2.3 \tag{15}$$

***For quadrupoles of cuboids**

Field: $32\gamma + 16\gamma + 8\gamma + 4\gamma + \gamma$ (5 types); threshold energy: $E_{photon} = 32\gamma = 12.9$ keV

$$Rate = \frac{5}{5\,\text{types}}\left[\frac{1}{1} + \frac{1}{4} + \frac{1}{8} + \frac{1}{16} + \frac{1}{32}\right] = 1.5 \tag{16}$$

Our results are collected in **Figure 1**.

Emphasize that the SST curve in **Figure 1** concerns the pure SST DM-BM interactions. Just we must apply some statistical methods to eliminate all other phenomena from our analyses.

The mean values of the DAMA/LIBRA and COSINE-100 selections are calculated on the basis of the data from [6].

The DAMA/LIBRA curve is consistent with the SST results for energies higher than 1.6 keV [5]. On the other hand, the SST and COSINE-100 results are consistent for energies higher than 3.2 keV. It suggests that statistical methods used in the COSINE-100 experiment for the region 1.6 keV up to 3.2 keV were not adequate.

Notice that a detector of photons must be at distance from the target bigger than the ranges of the created spacetime condensates.

For the weak interactions of DM-loops with BM via the virtual/real electron-positron pairs, for a target composed of atomic nuclei containing at least four cuboids (*i.e.* 32 nucleons), we have

$$DM_{loops} + BM \to E_i = N_i\gamma\,, \tag{17}$$

where $\gamma \approx 0.4$ keV, and $N_i = 1,4,8,16,32$, *i.e.* there are created 5 different entangled photons (5 types).

From formula (12) follows that for the interactions of DM with electrons (mass of the central condensate is a half of the bare mass of electron, *i.e.* about 1662 times lower than Y) we should observe a bump for photon energies equal to 0.243 eV. But cross sections for the DM-electron interactions are about 140

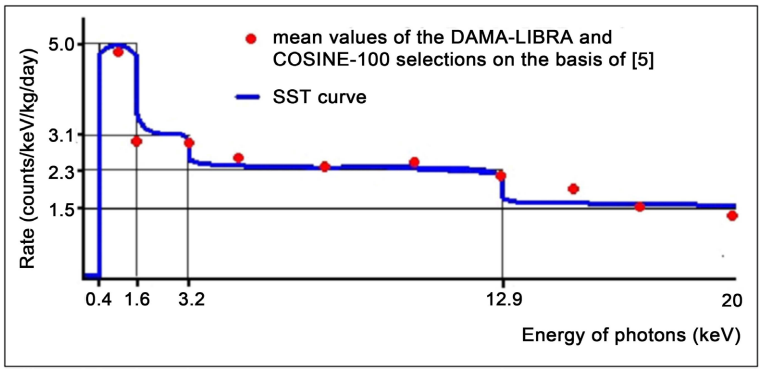

Figure 1. The SST dependence of the event rate on the photon energy in single-hit events.

times lower than for the DM-nucleon ones, so the rates for the single-hit events are much lower.

3. The Electron/Photon Interaction with a Solid Al

Notice that some deformed curve similar to the function *Rate* = *f*(*Energy*) for the DM-Solids interactions (see **Figure 1**) can appear for scattering of electrons/photons on very thin solids because then also appear the electron-positron pairs that can interact weakly with the Y spacetime condensates.

In such experiments (transmission of photons in 1 μm Al) [10] [11], for the interval from zero up to 2 keV, we obtain spectrums similar to the SST spectrum. Some comparison is presented in **Figure 2**.

We see that to detect DM we have to eliminate free electrons inside the baryonic matter used in the experiment, *i.e.* we have to use very good insulators (built of baryons) and screens that capture free electrons.

4. The SST DM-Baryon Interaction Cross-Section Normalized to Nucleon

The nuclear weak coupling constant, $\alpha_{w(p)} = 0.0187229$, relates to the radius of the Y spacetime condensate, $r_{C(p)} = 0.8711018 \times 10^{-17}\ \mathrm{m}$ [2]. On the other hand, effective radius of the condensate is directly proportional to coupling constant, so the cross-section for the SST DM-baryon interaction normalized to nucleon is

$$\sigma_{DM\text{-}baryon} = \pi\left(\frac{r_{C(p)} 2\alpha_{w(e)}}{\alpha_{w(p)}}\right)^2 = 2.46 \times 10^{-42}\ \mathrm{m}^2 = 2.46 \times 10^{-2}\ \mathrm{pb}. \tag{18}$$

The SST DM-nucleon cross-section, $\sigma_{DM\text{-}baryon} = 2.46 \times 10^{-2}\ \mathrm{pb}$, relates to the $Y = 0.4241\,\mathrm{GeV} \cdot \mathrm{c}^{-2}$ spacetime condensate that is the SST black hole because of the nuclear weak interactions (the weak black hole)

$$r_{C(p)} = \frac{G_w Y}{c^2}, \tag{19}$$

where $G_w = 1.0355025 \times 10^{27}\ \mathrm{m}^3 \cdot \mathrm{kg}^{-1} \cdot \mathrm{s}^{-2}$ is an analogue to the gravitational constant, G, for the nuclear weak interactions [2].

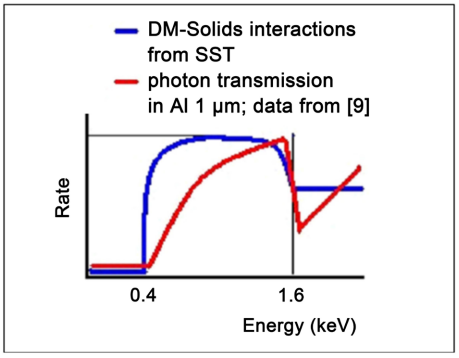

Figure 2. Some comparison of DM-Solids and Photon/Electron-Al interactions.

In cosmic spacetime, the Y, when separated from nuclear strong and electromagnetic interactions, behaves as a dark-matter particle, *i.e.* it interacts only weakly and gravitationally.

The SST values of $\sigma_{DM\text{-}baryon}$ and Y are very close but outside the NEWS-G (2017) constraints for dark-matter particle [12]. In [12] we have $\sigma_{excl} = 4.4\times10^{-41}\,\mathrm{m}^2$ for 0.5 GeV·c^{-2} and $\sigma_{excl} = 4.4\times10^{-43}\,\mathrm{m}^2$ for 16 GeV·c^{-2} WIMP excluded at 90% C.L. Our result is also very close but outside the CRESST-III 2019 constraints [13].

Emphasize that the SST DM loops have mass about 19 orders of magnitude lower than Y.

5. Rotation Curves of Disc Galaxies Outside Their Bulges

The inflows of DM into the spinning baryonic protogalaxies that were created inside the torus of the core of the Protoworld already before the beginning of the expansion of the Universe caused that the DM-loops absorbed most of angular momentum, so radii of them increased to cosmological scales. It means that density of DM in the bulges of massive spiral galaxies should be lower than outside them.

On the other hand, the weak interactions of BM with the DM loops (but also the other interactions of BM with the gluon/photon loops) caused that sizes of the baryonic discs increased and caused that some part of matter is in the intergalactic region.

The inflows of DM forced the collisions of the NBHs and the created nuclear plasma gathered on the equators of protogalaxies that radii were defined as follows

$$R_{beginning} = \frac{GM_{beginning}}{c^2}. \tag{20}$$

Moreover, in the nuclear-plasma rings were created the gluon loops that interacted strongly with nuclear plasma. Since the coupling constant for such interactions is $\alpha_s = v_{spin}/c = 1$ [2], so it additionally forced the spin speed of the nuclear-plasma rings to be close to c. But with time, due to the weak interactions

of BM with DM-loops, density of the nuclear plasma decreased, so there the DM-BM weak interactions started to dominate. It caused that radii of the BM rings increased to

$$R_{end} = R_{beginning} \frac{\alpha_s}{2\alpha_{w(e)}}. \tag{21}$$

Some part of the initial matter is outside the disc (*i.e.* $M_{end} < M_{beginning}$), so for the plateau region of the rotation curve we have

$$R_{end} = \frac{GM_{end}}{v_{spin}^2}, \tag{22}$$

where v_{spin} is the orbital speed of stars in the plateau region. Notice that for the plateau region the distribution of matter should satisfy the following relation: $M \sim r$. Such distribution results from the invariant mass of the DM loops (*i.e.* their mass does not depend on their radius) and from the constant distances between the concentric DM loops (it is due to a resonance because of the quantum entanglement). Notice that in SST, when we neglect the gravitational interactions of DM, the DM-DM interaction is due to the superluminal spin-1 entanglons that are responsible for the quantum entanglement – we can call them the dark photons.

From (20)-(22) we have

$$v_{spin} = c\left(\frac{2\alpha_{w(e)}M_{end}}{M_{beginning}}\right)^{\frac{1}{2}}. \tag{23}$$

Due to the pairing and the four-object symmetry, population of spiral binary systems composed of 8 protogalaxies, $M_{beginning} = 2\left(4M_{Proto,BM}\right) = 8.525\times10^{11}M_{Sun}$ was highest. Such object could transform into spiral galaxy or barred spiral galaxy.

The inflows of dark matter were chaotic, so the $\frac{M_{end}}{M_{beginning}}$ ratios can have different values for different galaxies even for galaxies with the same initial baryonic mass. But we see that applying formula (23) we can test our theory of dark matter. Just the observed orbital speed of stars in massive spiral galaxies in the plateau regions lead to the $\frac{M_{end}}{M_{beginning}}$ ratios, so using telescopes that can also observe the intergalactic baryonic matter, we can calculate both the M_{end} and $M_{beginning}$ to check whether formula (23) is correct.

By applying formula (23) we can calculate a mean orbital speed of stars in the plateau regions of the rotation curves for the massive spiral galaxies. The decay of $M_{beginning}$ into M_{end} and $\Delta M = M_{beginning} - M_{end}$ was realized in the massive galaxies in early Universe. Initially there were the NBHs in protogalaxies, but due to the massive inflows of DM loops, the massive spiral protogalaxies with the dominant mass of BH transformed into protogalaxies with the dominant mass of the accretion disc. In such accreting disc, the transitions from the

oscillations along the disc diameters (the wavelengths are $\lambda = 2r$) to the circular oscillations ($\lambda = 2\pi r$) decreased its initial mass $\frac{2\pi r}{2r} = \pi$ times. The ΔM was emitted via the BH jet and the BH accretion disc and today ΔM is scattered outside the entire radius of massive spiral galaxies (in the Milky Way Galaxy, it is outside the ring-like filament of stars called Triangulum-Andromeda Ring). It leads to a conclusion that the mean ratio, $\frac{M_{end}}{M_{beginning}}$, should be

$$\left(\frac{M_{end}}{M_{beginning}}\right)_{mean} = \frac{1}{\pi} = 0.31831, \tag{24}$$

so from formula (23) we obtain

$$v_{spin,mean} = 233\ \mathrm{km \cdot s^{-1}}. \tag{25}$$

We can compare it with observational data—they vary from ~120 km·s^{-1} (for example, NGC 6503 or NGC 2748) up to ~350 km·s^{-1} (for example, NGC 4984 or NGC 4594), so a mean is ~235 km·s^{-1}.

We see that a today mean entire baryonic mass of massive spiral galaxies should be $\sim 2.71\times10^{11} M_{Sun}$ while a today mean entire total mass (*i.e.* BM + DM) should be 6.39 times higher, *i.e.* $\sim 1.73\times10^{12} M_{Sun}$.

The lower limit for today entire total mass of massive galaxies (BM + DM) is 8 times lower than the mean mass because it concerns a single protogalaxy, *i.e.* we have $\sim 2.17\times10^{11} M_{Sun}$ (the lower limit for BM mass is $\sim 3.39\times10^{10} M_{Sun}$).

Initially spin speed of nuclear plasma on equator of BH was close to *c*. Spin speed is directly proportional to coupling constant, so for a transition from the strong interactions in cold nuclear matter ($\alpha_s^{NN,\pi} = 14.4$) to the nuclear weak interactions ($\alpha_{w(p)} = 0.0187229$) [2], we have

$$v_{spin,transition} = c\frac{\alpha_{w(p)}}{\alpha_s^{NN,\pi}} = 3.90\times10^{5}\ \mathrm{m \cdot s^{-1}}.$$

We define the entire radius of massive spiral galaxy as

$$R_{entire} = \frac{GM_{end}}{v_{spin,transition}^2}.$$

To the Milky-Way (MW) Galaxy we can apply the SST theoretical mean value $M_{beginning}/M_{end} = \pi$ because the orbital speeds of stars in the plateau region, *i.e.* $v_{spin} = 238 \pm 14\ \mathrm{km \cdot s^{-1}}$ [14], are consistent with the SST mean value 233 km·s^{-1}.

The arrangement of the arms of the Milky-Way MW Galaxy suggests that it started from 4 protogalaxies so the today baryonic mass of the entire MW should be

$$M_{BM,MW} = \frac{4M_{Proto\text{-}BM}}{\pi} = 1.36\times10^{11} M_{Sun}$$

while the total mass (BM + DM) of the entire MW should be

$$M_{end,MW} = 6.39 M_{BM,MW} = 0.87\times10^{12} M_{Sun}.$$

For the MW Galaxy we have $R_{entire,MW} = 24.6$ kpc —it is close to the radius of the ring-like filament of stars called Triangulum-Andromeda Ring.

We see that a mean entire radius of the massive spiral galaxies should be about 49 kpc.

6. Mean Dark-Matter-Halo (DMH) Mass around Quasars from SST

Most numerous should be quasars that were the binary systems of quadrupoles of the SST protogalaxies, *i.e.* the 8-protogalaxy quasars.

We see that a mean baryonic mass of quasars, $M_{BQ\text{-}mean}$, should be

$$M_{BQ\text{-}mean} = 8M_{Proto,BM} = 8.525\times10^{11}M_{Sun} = 5.8\times10^{11}h^{-1}M_{Sun}, \quad (26)$$

where the scaling factor for Hubble expansion rate from CMB anisotropies (Planck) is 0.674(5) [4], so for the distant quasars the value should be similar, *i.e.* $h \approx 0.68$ (a mean value should be 0.709).

On the other hand, SST shows that mass of dark matter is ~5.39 times higher than baryonic matter. We see that a mean DMH mass around quasars, $M_{DMH\text{-}quasar}$, should be

$$M_{DMH\text{-}quasar} = 5.39M_{BQ\text{-}mean} = 3.12\times10^{12}h^{-1}M_{Sun} \approx 10^{12.5}h^{-1}M_{Sun}. \quad (27)$$

On the other hand, the DMH mass of quasars is found to be nearly constant throughout cosmic time [15]

$$M_{DMH\text{-}quasar} \approx 10^{12.5}h^{-1}M_{Sun}. \quad (28)$$

We see that the SST result and observational data are in perfect agreement.

Moreover, SST shows that DMH masses of massive spiral galaxies that evolved from quasars are invariant. There is no mass evolution of DMHs—it is inconsistent with the assumption in mainstream cosmology. But emphasize that SST shows that initially, with time, the DMH sizes increased, *i.e.* the DMH masses are invariant but the DMH sizes increased.

According to SST, at the beginning of expansion of our Universe, there were inflows of the dark-matter (DM) loops into the baryonic protogalaxies composed of the SST neutron black holes. The DM loops "captured" the angular momentum of protogalaxies very easily, so the sizes of the DM loops grew rapidly and with them, due to the weak interactions, the sizes of the protogalaxies.

The tendency of matter to equalize the density of angular momentum throughout spacetime was the main driving force behind the evolution of protogalaxies. SST shows that the neutron black holes (NBHs) were created before the expansion of the Universe and initially dark matter and baryonic matter were separated. Next, the inflows of DM into BM forced collisions of the NBHs, so around the quasars were created the accretion discs containing nuclear plasma from NBHs. Dynamics of such quasars and growth of the DM halos transformed the quasars into the present-day massive spiral galaxies.

The black hole evaporation via the BH jet and accretion disc and how such a mechanism is coupled to the swelling of the DM halos we described in Section 9.

7. The Role of DM-Loops in Magnetars

The DM-loops with a radius of 16.915 km have spin equal to 1, so they should be in particular a stable objects, *i.e.* it should be very difficult to change their angular momentum and radius. Knowing that NBHs have mass 24.81 M_{Sun} and radius 36.64 km, we can calculate mass of neutron star (NS) with equatorial radius equal to 16.915 km—it is about 2.44 M_{Sun}, *i.e.* it is close to masses of magnetars. It suggests that the spin-1 DM-loops overlapping with equators of magnetars can have big influence on intensity of their magnetic fields.

Notice that the weak interactions of the spin-1 DM-loops with the equatorial plasma-vortices cause that the positively charged vortices are more stable, more massive and have higher density. Due to the interactions, periods of rotation of such vortices can be significantly shorter than the observed periods of magnetars, so intensity of magnetic fields should be much higher than other NSs.

For a number equilibrium of the DM-loops and neutrons and for a mass equilibrium of the DM-loops and the equatorial plasma vortex, we obtain that mass of the plasma vortex is

$$M_{plasma\text{-}vortex} = 6.027 \times 10^{10}\ \text{kg}. \tag{29}$$

High density of such plasma causes that there dominate the nuclei of helium-4, so the total electric charge, Q of the nuclear-plasma vortex is

$$Q = \frac{2eM_{plasma\text{-}vortex}}{4M_{Nucleon}} = 2.885 \times 10^{18}\ \text{C}. \tag{30}$$

The nuclear-plasma vortex can create the gluon loops, so a maximum spin speed of the vortex can be close to c. Then the period, T_P, of the vortex (not of magnetar) is

$$T_P > \frac{2\pi R_{Magnetar}}{c} = 3.5451 \times 10^{-4}\ \text{s}. \tag{31}$$

From the Biot-Savart law we have that the maximum value is

$$B_{Magnetar,DM,gluons,maximum} = \frac{\mu_o Q}{2R_{Magnetar}T_P} = 3.0 \times 10^{11}\ \text{T}. \tag{32}$$

In absence of the gluon loops, we have (see formula (23) for $M_{end} = M_{beginning}$)

$$T_{P,DM} = \frac{2\pi R_{Magnetar}}{c\sqrt{2\alpha_{w(e)}}} = 2.5704 \times 10^{-1}\ \text{s}. \tag{33}$$

Then from formula (32) we obtain the minimum value

$$B_{Magnetar,DM,minimum} = \frac{\mu_o Q}{2R_{Magnetar}T_{P,DM}} = 4.2 \times 10^{8}\ \text{T}. \tag{34}$$

On the other hand, from observational data we have [16]

$$6.1 \times 10^{8}\ \text{T} < B_{Magnetar,observed} < 2 \times 10^{11}\ \text{T}. \tag{35}$$

We can see a perfect consistency between our theoretical results and observational data.

A very high difference in the spin speeds of the nuclear-plasma vortex and the magnetar on its equator may lead to damages to the magnetar surface (solid crust) and therefore also may lead to short-lived bursts of energy.

8. Dark Matter in CMB

Both the three basic inflows of DM into baryonic plasma/matter during the collapse of the core of the Protoworld (it was built of the DM-tori that decayed to the DM-loops) and the atom-like structure of baryons are imprinted in the CMB.

Before the expansion of the Universe, the BM had concentrated on the circular axis [2] of the cosmological torus in the core of the Protoworld. It leads to a conclusion that during the collapse of the core there were three basic inflows of DM into BM. First inflow was due to the collapse of the cosmological torus towards its circular axis. The second one was during the expansion of the central condensate composed of DM, and the third one was because of the inflow from the opposite part of the cosmological torus.

Due to the three basic inflows of DM into BM, the baryonic matter was excited so it produced anisotropies in CMB that can be observed in the power spectrum. Just from the power spectrum of CMB we can decode the three basic inflows of DM and we can decode the atom-like structure of baryons. The excited internal structure of baryons in the initial nuclear plasma/matter, due to the expansion of the Universe, is now enlarged.

The weak interactions of the virtual electron-positron pairs in presence of DM lead to the present-day mean anisotropy power, $T_{a,mean}^2$

$$T_{a,mean}^2 = \left(T_{Universe}\alpha'_{w(e),DM}\right)^2 \approx \left(30.51\,\mu\mathrm{K}\right)^2 \approx 931\,\mu\mathrm{K}^2, \tag{36}$$

where $T_{Universe} = 2.7255(6)\,\mathrm{K}$ is the present-day temperature of the Universe [4], and $\alpha'_{w(e),DM} = 1.119446\times10^{-5}$ is the weak coupling constant for electrons in presence of DM [2].

Initially, the baryonic matter consisted of the neutron black holes which are the cold objects, so there dominated the nuclear strong interactions at low energy. Initially, the inflow of DM was not intensive so the protons and neutrons interacted due to the exchanged fundamental gluon loops between pions in the $d=1$ state. The coupling constant was $\alpha_s = \alpha_s^{\pi\pi,FGL} = 1$ [2] and the created virtual gluon loops had the radius equal to ($A+B$). Next there were the intensive inflows of the DM loops and creations of the alpha particles. Coupling constant for strongly interacting nucleons in atomic nuclei is $\alpha_s^{NN,\pi} = 14.40$ [2].

Lifetimes are inversely proportional to coupling constants so we can divide the angular scale (0˚ - 90˚) into two parts one related to the α_s (we denote it by $\Delta\varphi_{FGL}$) and the second one related to the $\alpha_s^{NN,\pi}$ (we denote it by $\Delta\varphi_\pi$)

$$\Delta\varphi_{FGL} = 90^\circ \frac{\alpha_s^{NN,\pi}}{\alpha_s^{NN,\pi}+\alpha_s} = 84.2^\circ \text{ i.e. } \varphi \text{ from } 90^\circ \text{ to } 5.8^\circ. \tag{37}$$

The definition which ties angular scale with multipole momentum, l, looks as

follows

$$l = \frac{180^\circ}{\varphi}, \tag{38}$$

so the SST plateau in CMB is from $l_{plateau,beginning} = 2$ to

$$l_{plateau,end} = \frac{180^\circ}{5.8^\circ} \approx 31. \tag{39}$$

We see that the SST plateau occupies almost whole angular scale so anisotropy power for the plateau should be only a little lower than the mean value. Assume that the plateau relates to the dark part of the Universe, so for the plateau we have

$$T_{plateau}^2 = \left[T_{a,mean}\left(h_{DM} + h_{DE}\right)\right]^2 \approx \left(29\ \mu\text{K}\right)^2 \approx 840\ \mu\text{K}^2. \tag{40}$$

Notice that the excitations of BM practically are defined by a triangle that relates to the first inflow of DM—we have (see **Figure 3**)

$$\frac{\sqrt{5600}\ \mu\text{K} - \sqrt{931}\ \mu\text{K}}{2} 5.8^\circ \approx 130.$$

It means that the plateau should be related to the dark part of the Universe and its anisotropy temperature should be below the mean value—we have (there is a rectangle)

$$\left(\sqrt{931}\ \mu\text{K} - 29\ \mu\text{K}\right)\left(90^\circ - 5.8^\circ\right) \approx 130.$$

What it means that the dark part of the Universe initially had an anisotropy temperature equal to ~29 μK? Just before the first inflow of DM, there was lower density of DM in BM but it was not equal to zero. Such DM gathered in the $d = 1$ state, *i.e.* $R_{d=1} = A + B$. There was the cold BM, *i.e.* the neutrons in the NBHs, so the coupling constant was $\alpha_s = 1$.

It is easy to calculate the anisotropy powers for the FGL and the TB orbits because from the Wien's displacement law results that temperature is inversely proportional to a peak radius R_{Peak} which here is equal to one of the TB radii or to the radius of FGL. The curve should peak for following anisotropy powers (emphasize that the plateau relates to $A + B$)

$$\frac{T^2}{T_{plateau}^2} = \left(\frac{A+B}{R}\right)^2. \tag{41}$$

Radius of the FGL is $R = 2A/3$ [2], so we have

$$T_{FGL}^2 = T_{plateau}^2 \left(\frac{A+B}{\frac{2A}{3}}\right)^2 \approx 5600\ \mu\text{K}^2. \tag{42}$$

It is for the biggest peak that was created due to the first most intensive inflow of DM.

For $R = A$ is

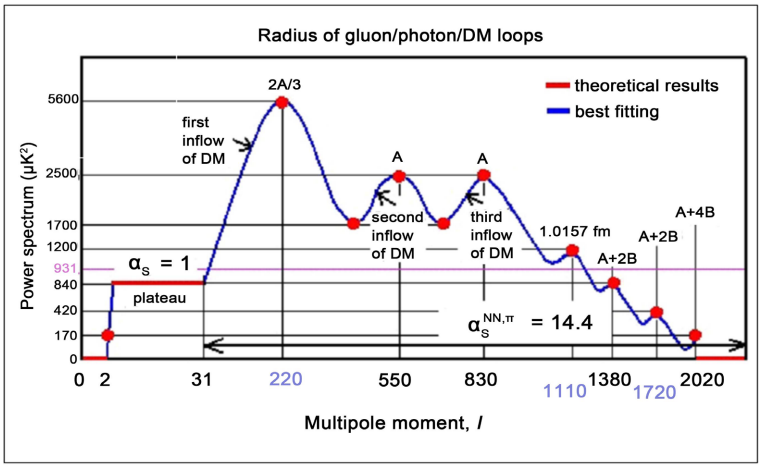

Figure 3. Theoretical results for CMB power spectrum from the atom-like structure of baryons for baryons interacting with dark-matter (DM) loops. Scales are not preserved.

$$T_A^2 = T_{plateau}^2 \left(\frac{A+B}{A}\right)^2 \approx 2500\ \mu\mathrm{K}^2 . \tag{43}$$

It is for the second and third peaks that were created due to the second and third less intensive inflows of DM. All the time the loops created in the distinguished states were scattered.

For $R = A + 2B$ is

$$T_{A+2B}^2 = T_{plateau}^2 \left(\frac{A+B}{A+2B}\right)^2 \approx 420\ \mu\mathrm{K}^2 . \tag{44}$$

For $R = A + 4B$ is

$$T_{A+4B}^2 = T_{plateau}^2 \left(\frac{A+B}{A+4B}\right)^2 \approx 170\ \mu\mathrm{K}^2 \tag{45}$$

We can see that the fourth peak does not relate to any TB orbit. It follows from the fact that for such a peak the energy was distributed among several orbits. Consider the first four orbits

$$R_{mean} = \frac{\frac{2A}{3} + A + (A+B) + (A+2B)}{4} = 1.0157\ \mathrm{fm} \tag{46}$$

For $R = R_{mean}$ is

$$T_{R-mean}^2 = T_{plateau}^2 \left(\frac{A+B}{R_{mean}}\right)^2 \approx 1200\ \mu\mathrm{K}^2 . \tag{47}$$

During the scattering of loops from the $d = 0$ state (*i.e.* $R = A$) they first of all gathered in distances equal to the muon radius of proton $R_{p(\mu)} = 0.8409(4)$ fm [4]. The anisotropy power for such distance is (it is a minimum)

$$T_{R-p(\mu)}^2 = T_{plateau}^2 \left(\frac{A+B}{R_{p(\mu)}}\right)^2 \approx 1700\ \mu\mathrm{K}^2 . \tag{48}$$

By applying a mixture of the SST theoretical results and observational data, we can indirectly show that the characteristic multipole moments in **Figure 3** relate to the characteristic radii that follow from the atom-like structure of baryons. We can calculate the increase in multipole moment per 1 MeV. Mass of the gluon loop in the $d=0$ state (*i.e.* $R=A$) is $S_{(+-o),d=0}\approx 727$ MeV [2]—it relates to $l_A=550$. Mass of the gluon loop in the $d=4$ state (*i.e.* $R=A+4B$) is $S_{(+-o),d=4}\approx 187$ MeV [2]—it relates to $l_{A+4B}=2020$. From it we have

$$F_{\Delta l/MeV}=\frac{2020-550}{727-187}=2.72\Delta l \text{ MeV}^{-1}. \tag{49}$$

Mass of the gluon loop in $A+B$ is $S_{(+-o),d=1}\approx 422$ MeV [2], so we have

$$l_{A+B}=l_{A+4B}-\left(S_{(+-o),d=1}-S_{(+-o),d=4}\right)F_{\Delta l/MeV}\approx 1380. \tag{50}$$

Mass of the gluon loop in $A+2B$ is $S_{(+-o),d=2}\approx 298$ MeV [2], so we have

$$l_{A+2B}=l_{A+4B}-\left(S_{(+-o),d=2}-S_{(+-o),d=4}\right)F_{\Delta l/MeV}\approx 1720. \tag{51}$$

Notice also that we should not observe anisotropy power for $l>l_{A+4B}=2020$ because the radius $A+4B$ is the radius of the last orbit—the angular scale for the upper limit of l is

$$\varphi_{A+4B}=\frac{180^\circ}{l_{A+4B}}=0.0891^\circ. \tag{52}$$

The same is for following angular scales: $0<\varphi<\left(90^\circ-\varphi_{A+4B}\right)$, so we should have no anisotropy power for following multipole moments:

$$\text{for } 0\le l<\sim 2 \text{ is } T^2=0. \tag{53}$$

Our results are in very good agreement with observational data [17].

In SST, the peaks in the CMB correspond to resonances in which the gluon/photon loops decouple from the characteristic orbits in baryons (*i.e.* there were perturbations of the density in the early Universe)—sizes of such loops are defined by the atom-like structure of baryons. In the expanding early Universe, decoupling of bigger loops was at lower densities of the nuclear plasma and DM. We can define such decoupling by modes that locate the peaks or by using an angular scale.

The spin polarization of the NBHs and protogalaxies created already before the collapse of the Protoworld leads to anomalous alignment while the four-object symmetry and saturation of interactions to non-Gaussian distribution.

The low amplitude for the quadrupole (l = 2) follows from the fact that initially there were the cold NBHs separated from DM—it is indeed the signature of new physics.

9. AGN Jet and Galactic-Halo Production

The inflows of the DM-loops into the two baryonic loops after the gravitational collapse of the core of the Protoworld forced collisions of the neutron black holes in protogalaxies, so nuclear plasma was created as an accretion disc around

spinning protogalaxy.

With time, the DM-loops took over most of angular momentum from accretion disc, so their radii increased. Due to the DM-BM weak interactions, there appeared radial motions of BM in plane of the accretion disc. Additionally, also due to the weak interactions of the DM-loops with the disc, spin speeds of the DM-loops decreased, so to conserve the resultant speed of the DM-loop components (*i.e.* the speed of light in "vacuum" c) there appeared motions of the concentric DM-loops (also of the gluon/photon loops and BM) in directions perpendicular to the plane of the disc. At greater and greater distances from the accretion disc, intensity of the DM-BM weak interactions was lower and lower, so the radial and perpendicular motions were damped. In such a way was created the flat/disc-like part of halos and DM-halos of the baryonic protogalaxies but emphasize that structure of the sphere-like part of galactic halos strongly depends also on the dynamics of the AGN jets.

Generally, due to the angular-momentum transfer, density of DM in the central bulge of the massive spiral galaxies should be lower.

We already explained why the mass of a galactic halo inside a concentric sphere is directly proportional to radius of the sphere ($M \sim r$). It means that outside the central bulge, the orbital speeds of stars, due to the gravitational interactions, should not depend on the distance from the centre of rotating galaxy. The same concerns the DM-BM weak interactions, so we can observe a resonance for orbital speeds forced by both the gravitational and weak interactions – it looks like an attractor with one stable state toward which a system tends to evolve.

Notice that such distribution of matter causes that for $r \gg r_{bulge}$, where r_{bulge} is the radius of the central bulge, the mean mass density in concentric sphere is inversely proportional to squared distance from galactic centre – it leads to the galactic gravitational lensing.

Emphasize that number of DM loops in our Universe and their mass are invariant but they can change their angular momentum, so also sizes. Under special conditions, solitons composed of the DM loops can be produced.

From SST we know that the surface mass density of the torus in the core of baryons is about 300,000 times higher than in the SST absolute spacetime, so in nuclear plasma with densities comparable with the densities in NBHs, angular momentums of both the plasma and the SST absolute spacetime are the same, *i.e.* the rotating plasma/NBH is practically in the rest in relation to the spacetime—it means that there does not appear relativistic mass and that spin speed of the DM/gluon/photon loops in relation to the spinning plasma is close to zero. It also means that the rotating BHs are not deformed, *i.e.* they behave as the BHs in the rest.

The DM loops placed inside the NBHs the BHs consist of have the relative spin speeds close to zero, so relativistic jets composed of DM loops are created (it concerns also the gluon/photon loops)—their weak interactions with baryons and leptons are responsible for dynamics of the protogalaxies.

AGN is super-massive black hole surrounded by accretion disc and dust torus and such a system is placed in centre of massive galaxy.

We can use the SST [2] to describe jet radius, R_{jet}, profile as a function of distance from centre of BH, L_{jet}. We define the jet radius as the distance between the boundary of jet and the jet axis (it is the radius of the jet emission) while the jet length as the axial distance from the centre/core of BH (in some articles, the L_{jet} is denoted by z).

Denote the gravitational radius of a black hole by $r_g = \frac{GM_{BH}}{c^2}$.

The DM loops and gluon/photon loops are moving along the jet axis of rotation and, due to the interactions of the loops, they drag matter.

Assume that the NBHs a BH consists of create a central condensate that emits the DM loops along the axis of rotation of the BH. A jet of such BH is created from matter inflowing to BH from accretion disc, so structure of the jet depends on the accretion disc. Assume that the BH produces fully developed jet. The inflowing plasma (from accretion disc to BH) creates inside BH a dynamical torus and dynamical condensate that partially overlaps with the central condensate in BH composed of the NBHs.

Due to a coupling constant α_i, a mass M can emit quanta with masses/energies equal to $\alpha_i M$ and range of such quanta is inversely proportional to mass/energy of them, *i.e.*

$$\frac{R_1}{R_2} = \frac{L_1}{L_2} = \frac{\alpha_2 M}{\alpha_1 M} = \frac{\alpha_2}{\alpha_1}. \tag{54}$$

From SST follows that in baryons, the electron and electron-antineutrino appear on the circular axis, so in BH, the initial electron-jet radius relates to

$$R_{o,jet(e)} = \frac{2r_g}{3} \approx 0.667\left[r_g\right]. \tag{55}$$

Next, the transitions from the radial oscillations to circular/poloidal oscillations cause that the initial electron-jet length is 2π times lower

$$L_{0,jet(e)} = \frac{R_{o,jet(e)}}{2\pi} \approx 0.106\left[r_g\right]. \tag{56}$$

We see that the electron jet starts from the electron loop with the toroidal radius equal to $0.667\left[r_g\right]$ and the poloidal radius equal to $0.106\left[r_g\right]$.

On the BH circular axis, the spin speed is equal to c so we can normalize the electron-jet length and electron-jet radius via the nuclear strong interactions (S) of the FGLs at low energies, *i.e.* $2r_g/3$ relates to $\alpha_s = 1$. From (54) follows that a transition from some interactions defined by the coupling constant at a beginning, $\alpha_{beginning}$, to some interactions defined by the coupling constant at an end, α_{end}, causes that the jet radius or jet length changes $\frac{\alpha_{end}}{\alpha_{beginning}}$ times. Moreover, the nuclear strong interactions dominate in the directions perpendicular to the spins of baryons whereas the nuclear weak interactions dominate along the di-

rections of spins of them. On the other hand, spins of fermions should be parallel (or antiparallel) to the toroidal velocities, so L_{jet} relates to $\alpha_{beginning}=\alpha_s$ while R_{jet} relates to $\alpha_{beginning}=\alpha_{w(p)}=0.0187229$ that is the coupling constant for the nuclear weak interactions (W(p)) via the Y spacetime condensates.

Such remarks lead to

$$L_{jet(e),transition}=\frac{\alpha_s}{\frac{\alpha_{end}}{\alpha_{beginning}}}\frac{2r_g}{3}=\frac{2\alpha_s}{3\alpha_{end}}r_g, \tag{57}$$

$$R_{jet,transition}=\frac{\alpha_s}{\frac{\alpha_{end}}{\alpha_{beginning}}}\frac{2r_g}{3}=\frac{2\alpha_{w(p)}}{3\alpha_{end}}r_g. \tag{58}$$

Notice that to increase sizes of the BH jet, the transitions must be from stronger to weaker interactions.

Along the jet axis there can be the transition $\alpha_s\to\alpha'_{w(e),DM}$, where $\alpha'_{w(e),DM}=1.1194\times10^{-5}$ is the coupling constant for the weak interactions of the electrons in presence of DM (W(e, DM)). From (57), we obtain

$$L_{jet(e),length,S\to W(e,DM)}=\frac{2\alpha_s}{3\alpha'_{w(e),DM}}r_g=0.5955\times10^5\left[r_g\right]. \tag{59}$$

Simultaneously, in direction perpendicular to the jet axis there can be the transition $\alpha_{w(p)}\to\alpha'_{w(e),DM}$. From (58), we obtain

$$R_{jet(e),radius,W(p)\to W(e,DM)}=\frac{2\alpha_{w(p)}}{3\alpha'_{w(e),DM}}r_g=1.1150\times10^3\left[r_g\right]. \tag{60}$$

The formulae (55), (56), (59) and (60) for the electron jet lead to following equation that relates the electron-jet radii to electron-jet lengths expressed in $\left[r_g\right]$

$$\log R_{jet(e)}=0.56067\log L_{jet(e)}+0.37015. \tag{61}$$

Along the jet axis there can be the transition $\alpha_s\to\alpha_{w(e)}$, where $\alpha_{w(e)}=0.9511182\times10^{-6}$ is the coupling constant for the *local* weak interactions of protons with electrons (W(e)), so it concerns the proton jet. But notice that initially the baryonic matter accumulates on the BH equator, so r_g relates to $\alpha_s=1$. From (57) we have

$$L_{jet(p),length,S\to W(e)}=\frac{\alpha_s}{\alpha_{w(e)}}r_g=1.0514\times10^6\left[r_g\right]. \tag{62}$$

Simultaneously, in direction perpendicular to the jet axis, there can be the transition $\alpha_{em}\to\alpha_{w(e)}$, where $\alpha_{em}=1/137.036$ is the coupling constant for the electromagnetic interactions (EM). There appears the fine structure constant, α_{em}, because in the initial state of the proton jet there is $\alpha_{w(p)}+\alpha_{em}$ (see formula (65)) and $\alpha_{em}<\alpha_{w(p)}$, so there is the transition $\alpha_{w(p)}+\alpha_{em}\to\alpha_{em}$. From (58), we obtain

$$R_{jet(p),radius,EM\to W(e)}=\frac{\alpha_{em}}{\alpha_{w(e)}}r_g=0.76724\times10^4\left[r_g\right]. \quad (63)$$

Initially baryonic matter appears on the BH equator but as follows from the dynamics of the core of baryons described in SST [2], there is transition from radial oscillations to circular oscillations, so the initial toroidal radius of the baryonic loop is

$$R_{0,jet(p)}=\frac{r_g}{2\pi}\approx0.159\left[r_g\right]. \quad (64)$$

From (57) follows that due to the transition from the nuclear strong interactions to the simultaneous nuclear-weak and electromagnetic interactions along the jet axis, such baryonic loop has the range

$$L_{0,jet(p)}=\frac{\alpha_s}{\alpha_{w(p)}+\alpha_{em}}r_g=38.43\left[r_g\right]. \quad (65)$$

We see that the proton/baryonic jet starts from the baryonic pipe with the toroidal radius equal to $0.159\left[r_g\right]$ and the length equal to $38.43\left[r_g\right]$, so at distance $38.43\left[r_g\right]$ we should observe higher density of baryonic matter.

The formulae (62)-(65) for the proton jet lead to following equation that relates the proton-jet radii to proton-jet lengths expressed in $\left[r_g\right]$

$$\log R_{jet(p)}=1.05545\log L_{jet(p)}-2.47074. \quad (66)$$

For the point of intersection, *i.e.* then the proton-jet radius and electron-jet radius are the same, the distributions of protons and electrons are similar, so the local electroweak (EW) interactions are saturated to a maximum. We see that at the point of intersection the magnetic field has lower intensity so it can lead to the magnetic kink instability. From (61) and (66) we obtain:

$L_{intersection}=0.552\times10^6\left[r_g\right]$, $R_{intersection}=0.388\times10^4\left[r_g\right]$, and $\frac{L_{intersection}}{R_{intersection}}=142$.

From it follows that for $L_{jet}<L_{intersection}$, the proton jet lies inside the electron jet while for $L_{jet}>L_{intersection}$, the electron jet lies inside the proton jet – it is the origin of the transition from the parabolic to conical shape of the jet.

Our results are collected in **Figure 4**—they are consistent with observational data [18] [19]. Emphasize that to describe the jet profiles we used only the coupling constants and initial conditions that follow from the atom-like structure of baryons [2].

In SST, the corona-jet model looks as follows. Some amount of the cold nuclear plasma appears on the circular axis of BH. For the transition $\alpha_s^{NN,\pi}\to\alpha_s$, where $\alpha_s^{NN,\pi}=14.40$ is the coupling constant for the strong interactions of the cold nuclear matter, we obtain that the distance between the BH centre and the corona, H_{corona}, is $H_{corona}=\frac{\alpha_s^{NN,\pi}}{\alpha_s}\frac{2r_g}{3}=9.6\left[r_g\right]$, *i.e.* $\log\frac{H_{corona}}{r_g}=0.98$—it is consistent with observational data [20]. The corona radius we can calculate from (61): $R_{corona}=8.3\left[r_g\right]$.

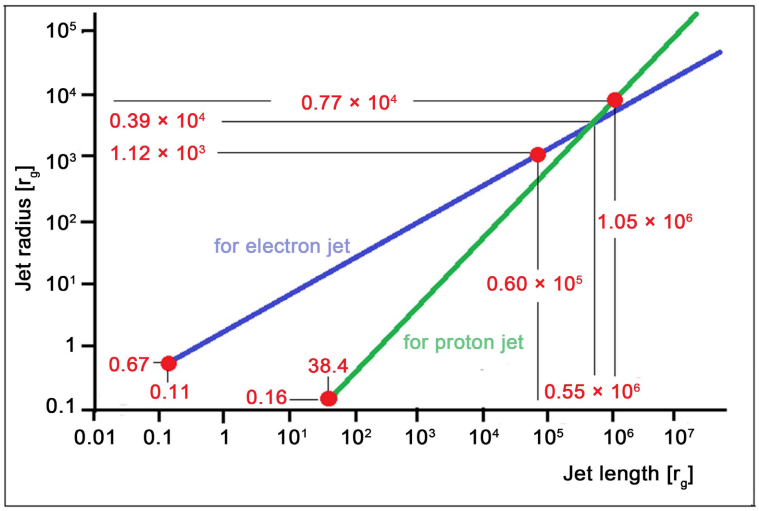

Figure 4. The SST jet radius as a function of jet length.

On the circular axis and/orequator of BH (*i.e.* in plane perpendicular to the BH axis of rotation) there can be created one baryon loop or two baryon loops with opposite internal helicities. One loop creates one half-jet while two loops create two half-jets moving in opposite directions.

The loops emitted along the axis of jet, due to their interactions with plasma, accelerate the plasma, take over angular momentum so they increase the jet radius (it stretches the collimated jet), and collimate the jet.

The spin velocities of the DM/gluon/photon loops force the toroidal motions of plasma and force the radial motion along the jet axis. Additionally, the gluon/photon loops force the poloidal motions around the loops.

To describe the streamlines of the jets, we can use the following relation

$$L_{jet} = bR_{jet}^{a}, \tag{67}$$

where b and a are some parameters. The parameter a defines the *jet* shape.

From (61), for the electron jet we have

$$L_{jet(e)} = 0.219R_{jet(e)}^{1.7836}. \tag{68}$$

From (66), for the proton jet we have

$$L_{jet(p)} = 219R_{jet(p)}^{0.9475}. \tag{69}$$

From (68) we have $a = 1.7836 \approx 1.78$, so it is a parabolic shape of the electron jet while from (69) we have $a = 0.9475 \approx 0.95$, so it is a conical shape of the proton jet—both results are consistent with observational data [19] (see **Figure 5**): $a = 1.73 \pm 0.05$ and $a = 0.96 \pm 0.10$ respectively.

As a conclusion we can say that when a gravitational BH is surrounded by a nuclear accretion disc then inside such BH the other interactions appear. The DM/gluon/photon loops with lower spin speed are moving along axis of rotation, so they drag matter. Initially, relativistic mass of dragged matter increases but next the relativistic mass and angular momentum of dragged matter decrease while spin speed and radius of the loops increase.

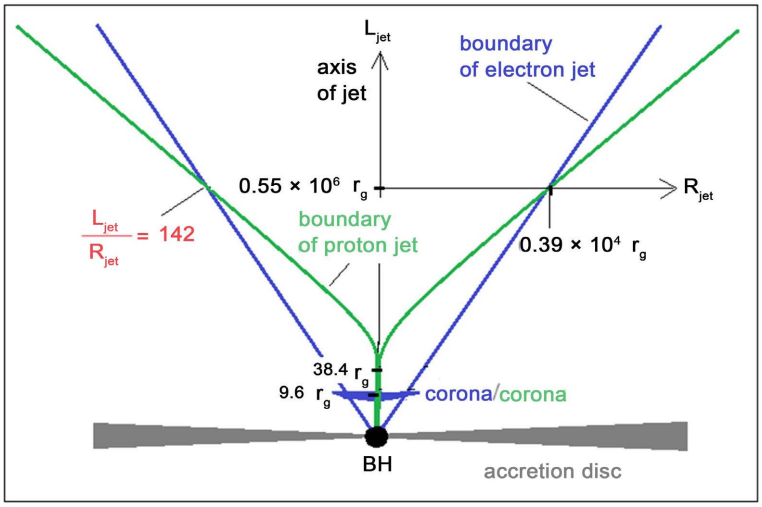

Figure 5. Fully developed proton-jet (green) and electron-jet (blue) in logarithmic scale.

10. Summary

In baryons, the DM-loops must pass through the Y spacetime condensate—then the weak DM-Y interaction via a virtual/real electron-positron pair is possible. Such interaction is local so instead the coupling constant $2\alpha'_{w(e),DM}$ that is for the global weak interactions of electrons (then wave function must occupy whole spacetime), we have $2\alpha_{w(e)}$ that value is about 11.77 times lower [2].

The spacetime condensates with energy $2\alpha_{w(e)}Y = 0.807$ keV (the photons with energy ~0.4 keV) are created due to the SST local weak interactions. Due to the four-particle symmetry and the energy equilibrium, there appear also associations of the photons that lead to the characteristic spectrum for the DM-BM interactions.

The averaged function describing the dependence of the event rate on the photon energy in single-hit events obtained in the DAMA/LIBRA and COSINE-100 experiments for energies higher than 1 keV is consistent with the curve obtained in this paper. It suggests that the DAMA/LIBRA team indeed discovered the DM-BM interactions—notice that here such a conclusion is not related to the annual modulation.

Let us also emphasize that in both the LIBRA/DAMA and COSINE-100 experiments, contrary to SST, the region from zero to 1 keV was not studied in detail, so we can verify the SST DM model.

We showed that the origin of dark matter described in SST leads to the observational and experimental data—it concerns the mean DMH mass of quasars, rotational curves of massive spiral galaxies, the averaged DAMA/LIBRA/COSINE-100 curve describing the dependence of the event rate on the photon energy in single-hit events, the magnetic fields of magnetars, the CMB power spectrum, AGN-jet production and galactic-halo production.

We also widely described properties of dark energy—it cannot be detected directly because DE concerns the virtual fields. When a gravitational mass col-

lapses then the negative pressure from DE increases. Emphasize that the two dominant masses/energies in the expanding Universe, *i.e.* the total energy of DE and total mass of DM, are invariant. The origin of DE leads to an acceleration of the initial expansion of both the baryonic mass and DM in the early Universe.

We do not need dark energy to explain the observed increase in the expansion rate (the Hubble tension) that is a result of a change in value of the coupling constant for the nuclear strong fields during the initial stages of the expansion of the Universe.

SST shows that expanding spacetime should have a significant influence on the values of the physical constants c and G. Especially the G should change rapidly. We do not observe it, so the mainstream assumption that the ground state of the absolute spacetime expands is incorrect. Moreover, our Universe is flat, so mass density of the ground state of the SST absolute spacetime must dominate. Therefore, why, globally, we do not observe the relativistic masses of galaxies? Destruction of the neutron-like structure of the Protoworld started the expansion of the Universe. Due to the superluminal quantum entanglement, dark matter and other matter and dark energy (DE is a result of the SST dynamics of virtual field) are mutually entangled. The galaxies are not entangled with the ground state of the SST absolute spacetime but with the dark part of the Universe, so, globally, relative speed of the galaxies in relation to the dark part of the Universe is zero—it explains why we do not observe the relativistic masses of galaxies.

Conflicts of Interest

The author declares no conflicts of interest regarding the publication of this paper.

References

[1] Corda, C. (2009) Interferometric Detection of Gravitational Waves: The Definitive Test for General Relativity. *International Journal of Modern Physics D*, **18**, 2275-2282. https://doi.org/10.1142/S0218271809015904

[2] Kornowski, S. (2024) Foundations of the Scale-Symmetric Theory and the Illusory Total Width of the Off-Shell Higgs Bosons. *Journal of High Energy Physics, Gravitation and Cosmology*, **10**, 398-437. https://doi.org/10.4236/jhepgc.2024.101028

[3] Palanque-Delabrouille, N., *et al.* (2020) Hints, Neutrino Bounds, and WDM Constraints from SDSS DR14 Lyman-α and Planck Full-Survey Data. *Journal of Cosmology and Astroparticle Physics*, **4**, 38. https://doi.org/10.1088/1475-7516/2020/04/038

[4] Workman, R.L., *et al.* (2022) Review of Particle Physics. *Progress of Theoretical and Experimental Physics*, **2022**, 083C01. https://doi.org/10.1093/ptep/ptac097

[5] Bernabei, R., *et al.* (2019) Improved Model-Dependent Corollary Analyses after the First Six Annual Cycles of DAMA/LIBRA-Phase2. *Nuclear Physics and Atomic Energy*, **20**, 317-348. https://doi.org/10.15407/jnpae2019.04.317

[6] Adhikari, G., Carlin, N., Choi, J., *et al.* (2023) An Induced Annual Modulation Signature in COSINE-100 Data by DAMA/LIBRA's Analysis Method. *Scientific Re-*

ports, **13**, Article No. 4676.

[7] de Barbosa Souza, E., *et al.* (2017) First Search for a Dark Matter Annual Modulation Signal with NaI(T*l*) in the Southern Hemisphere by DM-Ice17. *Physical Review D*, **95**, Article ID: 032006. https://doi.org/10.1103/PhysRevD.95.032006

[8] Amaré, J., *et al.* (2019) First Results on Dark Matter Annual Modulation from ANAIS-112 Experiment. *Physical Review Letter*, **123**, Article ID: 031301. https://doi.org/10.1103/PhysRevLett.123.031301

[9] Antonello, M., *et al.* (2019) The SABRE Proof-of-Principle. *The European Physical Journal C*, **79**, 363.

[10] Shimizu, R., *et al.* (1976) A Monte Carlo Approach to the Direct Simulation of Electron Penetration in Solids. *Journal of Physics D: Applied Physics*, **9**, Article 101. https://doi.org/10.1088/0022-3727/9/1/017

[11] Agostinelli, S., et al. (2003) GEANT4—A Simulation Toolkit. *Nuclear Instruments and Methods in Physics Research A*, **506**, 250-303.

[12] Arnaud, Q., *et al.* (2018) First Results from NEWS-G Direct Dark Matter Search Experiment at the LSM. *Astroparticle Physics*, **97**, 54-62. https://doi.org/10.1016/j.astropartphys.2017.10.009

[13] Abdelhameed, H., *et al.* (2019) First Results from the CRESST-III Low-Mass Dark Matter Program. arXiv: 1904.00498v1.

[14] Honma, M., *et al.* (2012) Fundamental Parameters of the Milky Way Galaxy Based on VLBI Astronomy. *Publications of the Astronomical Society of Japan*, **64**, Article 136.

[15] Arita, J., *et al.* (2023) Subaru High-z Exploration of Low-luminosity Quasars (SHELLQs). XVIII. The Dark Matter Halo Mass of Quasars at z~6. *The Astrophysical Journal*, **954**, Article 210. https://doi.org/10.3847/1538-4357/ace43a

[16] Olausen, S.A. and Kaspi, V.M. (2014) The McGill Magnetar Catalog. *The Astrophysical Journal Supplement*, **212**, Article 6. https://doi.org/10.1088/0067-0049/212/1/6

[17] Planck Collaboration (2020) Planck 2018 Results. V. CMB Power Spectra and Likelihoods. arXiv: 1907.12875v2.

[18] Hada, K. (2019) Relativistic Jets from AGN Viewed at Highest Angular Resolution. Galaxies, **8**, Article 1. https://doi.org/10.3390/galaxies8010001

[19] Asada, K. and Nakamura, M. (2012) The Structure of the M87 Jet: A Transition from Parabolic to Conical Streamlines. *The Astrophysical Journal Letters*, **745**, L28. https://doi.org/10.1088/2041-8205/745/2/L28

[20] King, A.L., Lohfink, A. and Kara, E. (2017) AGN Coronae through a Jet Perspective. *The Astrophysical Journal*, **835**, Article 226. https://doi.org/10.3847/1538-4357/835/2/226